Inverse SAR Imaging of Circularly and Linearly Polarized Synthetic Aperture Radar

Yuta Izumi1, Sevket Demirci2, Mohd Zafri Baharuddin1, and Josaphat Tetuko Sri Sumantyo1
1Center for Environmental Remote Sensing, Chiba University, Chiba 263-8522 Japan
2Electrical and Electronic Faculty of Engineering, Mersin University, Yenisehir, Mersin 33343 Turkey

***Abstract* – C-band, 4-8 GHz, inverse synthetic aperture radar (ISAR) experiments have been conducted to investigate the characteristics of a proposed synthetic aperture radar (SAR) system using circularly polarized antennas. The aluminum plate and dihedral reflectors were selected as targets to analyze the difference of scattering between odd-numbered and even-numbered bounce. SAR measurements with linearly polarized antennas were also performed for comparison. The SAR images show clear differences between co-polarization and cross-polarization setup of the antenna, and is consistent with theory.**

***Index Terms* —Circular polarization, inverse synthetic aperture radar, synthetic aperture radar.**

1. Introduction

Circularly polarized (CP) antennas were chosen due to advantages in negligibly small effect on the antenna orientation, multi-scattering, and weather clutter reduction [1]. This paper focuses on the remote sensing application of CP antennas for Earth surface monitoring synthetic aperture radar (SAR). To test the performance of CP-SAR, a full-polarimetric inverse SAR (ISAR) test was conducted in an anechoic chamber. For comparison, linearly polarized (LP) SAR experiments were also made using the same arrangement. The experiment utilizes a vector network analyzer (VNA), CP and LP antennas, a control computer, and two canonical corner reflectors; an aluminum plate and a horizontal dihedral.

2. Circular Polarization Characteristic

The basis of the Sinclair scattering matrix can be transformed from LP to CP using following equation [2]

$$\begin{bmatrix} S_{LL} & S_{LR} \\ S_{RL} & S_{RR} \end{bmatrix} = \frac{1}{2}\begin{bmatrix} 1 & j \\ j & 1 \end{bmatrix}\begin{bmatrix} S_{HH} & S_{HV} \\ S_{VH} & S_{VV} \end{bmatrix}\begin{bmatrix} 1 & j \\ j & 1 \end{bmatrix}, \quad (1)$$

where L and R are left-handed circular polarization (LHCP) and right-handed circular polarization (RHCP) respectively. For convenience, this paper defines the scattering order as reception and transmission. The scattering matrices with CP basis for single bounce and double bounce are derived from (1) with the results expressed as (2) and (3).

$$\begin{bmatrix} S_{LL} & S_{LR} \\ S_{RL} & S_{RR} \end{bmatrix} = \begin{bmatrix} 0 & j \\ j & 0 \end{bmatrix} \text{ (single bounce)}, \quad (2)$$

$$\begin{bmatrix} S_{LL} & S_{LR} \\ S_{RL} & S_{RR} \end{bmatrix} = \begin{bmatrix} 1 & 0 \\ 0 & -1 \end{bmatrix} \text{ (double bounce)}. \quad (3)$$

3. Experiment

The ISAR setup was chosen to perform CP and LP SAR measurements. Spiral cone antennas were used for CP whereas horn antennas were used for LP. The target moves linearly along a 2.2-meter-long rail that was set 4.2 meter away from the antenna. The movement is controlled by a computer which also triggers the VNA to transmit and receive the RF signals as shown in Fig. 1. This experiment was conducted using a stop-and-go method where the target stops at each azimuth interval along the azimuth length. A flat plate (600 x 900 mm) and horizontal dihedral (600 x 600 x 900 mm) made from aluminum were selected as the target reflector. The flat plate and dihedral have scattering characteristics of single bounce and double bounce respectively. Thus these ideal scattering matrices are defined as (2) and (3). The back-projection algorithm was applied for SAR image processing [3]. The experimental parameters are shown in Table I.

TABLE I
Specification of circularly polarized SAR

Category	Specification
Axial ratio (cone antenna) [dB]	< -0.5
Frequency range [GHz]	4~8
Number of pulse	101
Output power [dBm]	5

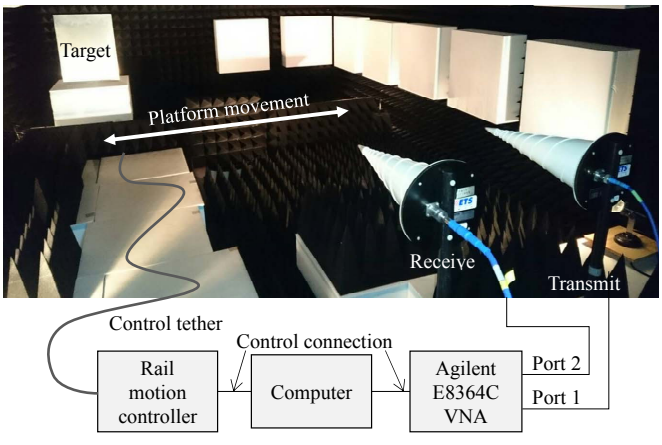

Fig. 1. The target reflector and circularly polarized-antennas set-up inside an anechoic chamber.

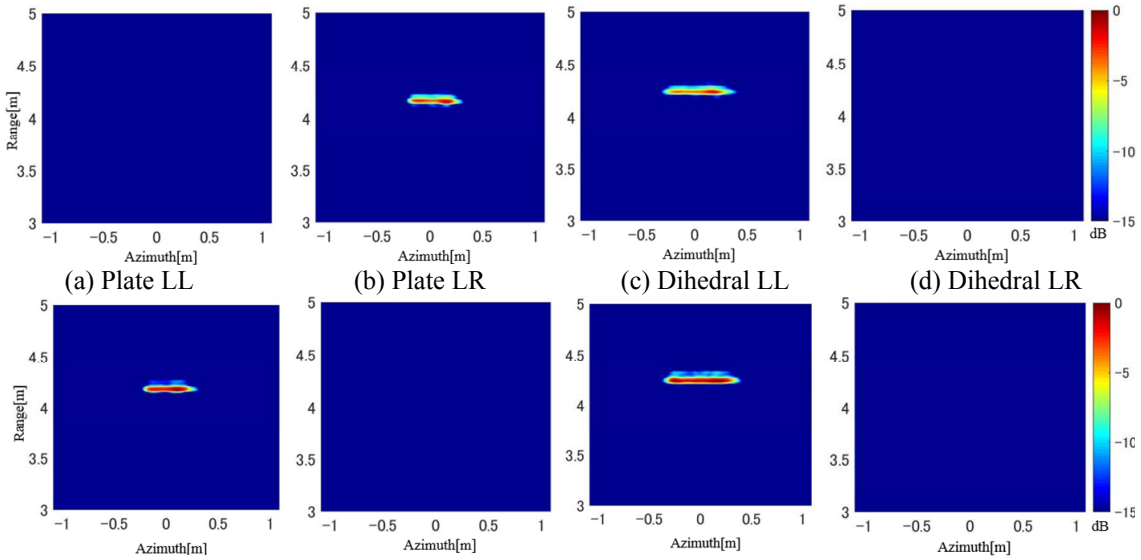

(a) Plate LL (b) Plate LR (c) Dihedral LL (d) Dihedral LR

(e) Plate HH (f) Plate HV (g) Dihedral HH (h) Dihedral HV

Fig. 2. Output SAR images after back-projection processing. Figures (a)-(d) show CP-SAR configuration results. Figures (e)-(h) show LP-SAR configuration results.

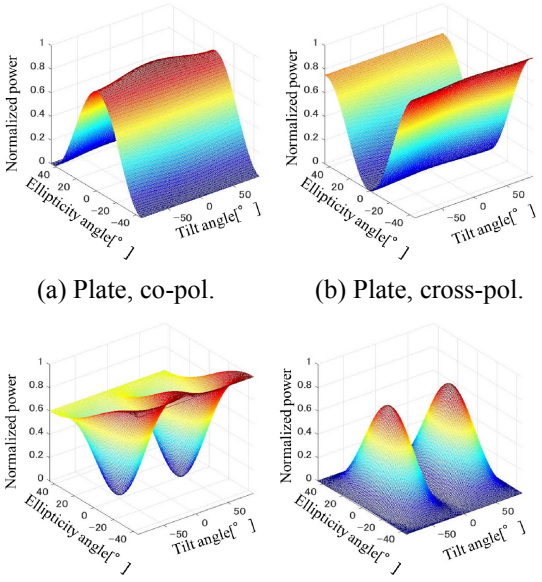

(a) Plate, co-pol. (b) Plate, cross-pol.

(c) Dihedral, co-pol. (d) Dihedral, cross-pol.

Fig. 3. Polarimetric signatures generated from circularly polarized-SAR measurement.

4. Experimental Results

SAR images generated from the ISAR experiment are shown in Fig. 2. The images in Fig. 2 are normalized to the maximum signal strength in one set of polarization. The measured scattering matrices are taken from the center of images as follows:

$$\begin{bmatrix} S_{LL} & S_{LR} \\ S_{RL} & S_{RR} \end{bmatrix} = \begin{bmatrix} 0.063 & 0.865 \\ 1 & 0.03 \end{bmatrix} \quad \text{(CP Plate)}, \qquad (4)$$

$$\begin{bmatrix} S_{LL} & S_{LR} \\ S_{RL} & S_{RR} \end{bmatrix} = \begin{bmatrix} 0.774 & 0.06 \\ 0.043 & 1 \end{bmatrix} \quad \text{(CP Dihedral)}, \qquad (5)$$

$$\begin{bmatrix} S_{HH} & S_{HV} \\ S_{VH} & S_{VV} \end{bmatrix} = \begin{bmatrix} 1 & 0.0197 \\ 0.034 & 1 \end{bmatrix} \quad \text{(LP Plate)}, \qquad (6)$$

$$\begin{bmatrix} S_{HH} & S_{HV} \\ S_{VH} & S_{VV} \end{bmatrix} = \begin{bmatrix} 1 & 0.089 \\ 0.113 & 0.959 \end{bmatrix} \quad \text{(LP Dihedral)}. \qquad (7)$$

Equations (4)-(7) are normalized to 1. The measured scattering matrices are similar to the ideal scattering matrix. To perform additional analysis, the CP-SAR polarimetric signature was calculated from each scattering matrix and shown in Fig. 3. Some distortions are seen in the measured polarimetric signatures. This suggests the necessity for appropriate CP and LP polarimetric calibration.

5. Conclusion

This paper presents the CP and LP SAR experiment using VNA and canonical reflectors in an anechoic chamber. The SAR imaging of CP and LP is achieved but the polarimetric signature of CP-results includes some distortions. Although the experimental scattering matrices have approximately the same characteristics, polarimetric calibrations for both CP-SAR and LP-SAR are required. This work is step towards the development of a CP-SAR onboard satellite in the future.

Acknowledgment

This work was supported by the Japanese Ministry of Education and Technology (Monbukagakusho); Japan Int'l Cooperation Agency (JICA) and Kazuyuki Saito.

References

[1] A. Kajiwara, "Line-of-sight indoor radio communication using circular polarized waves," in *IEEE Transactions on Vehicular Technology*, vol. 44, no. 3, pp. 487-493, Aug 1995.

[2] Y. Yamaguchi, *Radar polarimetry from Basics to Applications: Radar Remote Sensing using Polarimetric Information*. IEICE: Tokyo, 2007, pp.82-84.

[3] S. Demirci, H. Cetinkaya, E. Yigit, C. Ozdemir, and A. A. Vertiy, "A study on millimeter-wave imaging of concealed objects: application using back-projection algorithm," *Progress In Electromagnetics Research*, Vol. 128, pp. 457-477, 2012.